The Cryosphere Discuss., 3, 1023–1068, 2009
www.the-cryosphere-discuss.net/3/1023/2009/

The Cryosphere Discussions

This discussion paper is/has been under review for the journal The Cryosphere (TC).
Please refer to the corresponding final paper in TC if available.

Polynyas in a dynamic-thermodynamic sea-ice model

E. Ö. Ólason and I. Harms

Centre for Marine and Atmospheric Research, Institute of Oceanography, University of Hamburg, Hamburg, Germany

Received: 28 October 2009 – Accepted: 9 November 2009 – Published: 24 November 2009

Correspondence to: E. Ö. Ólason (einar.olason@zmaw.de)

Published by Copernicus Publications on behalf of the European Geosciences Union.

Abstract

The response of a viscous-plastic dynamic-thermodynamic sea-ice model to a constant wind forcing is tested in an idealised setting. Bjornsson et al. (2001) have shown that the granular model of Tremblay and Mysak (1997) gives good results in such a set-up compared to a polynya flux model. Here it is shown that these results can be duplicated using the computationally more efficient elliptic yield curve approach by Hibler (1979) and modified Coulombic yield curve by Hibler and Schulson (2000). Some care is, however, required regarding the parametrisations of the ellipse. In addition it is shown that the new ice thickness formulation of Mellor and Kantha (1989) does not allow for proper polynya formation in the bay. In contrast the new ice thickness formulation of Hibler (1979) is found to give good results. Finally we propose a parametrisation of the ice demarcation thickness (h_0) in Hibler's formulation, based on wind speed and ice thickness.

1 Introduction

One of the most interesting features of sea-ice, in a climate context, is the fact that it acts as an insulating layer between the atmosphere and ocean. As the ice grows, the transfer of heat from ocean to atmosphere is greatly reduced. This slows down further ice formation and allows the atmosphere to cool much more than it otherwise would.

This blanket of ice is of course subject to atmospheric and oceanic forcing, which can create openings in the cover that again allow direct heat exchange between the ocean and the atmosphere. Where this happens, the heat transfer may increase up to hundredfold causing vigorous ice formation, brine release and heating of the atmosphere near the opening. In the present context these openings are either small fractures or leads, or larger openings referred to as polynyas.

Polynyas and leads are an important part of the climate system at high latitudes. Maykut (1982), for instance, estimates that in winter about 50% of the total atmosphere-

TCD

3, 1023–1068, 2009

ocean heat exchange over the Arctic Ocean occurs through polynyas and leads. During summer these openings admit shortwave radiation into the ocean, warming it up and thus impacting the heat and mass balance of the ice and ocean (Maykut and Perovich, 1987; Maykut and McPhee, 1995). Arctic polynyas also play a large role in halocline and deep water formation and Winsor and Björk (2000) estimate a mean ice production from all Arctic polynyas of $300 \pm 30 \mathrm{km}^3\,\mathrm{yr}^{-1}$. The resulting salt flux is about 30% of the estimated flux needed to maintain the halocline.

Most of the ice formation and brine expulsion in polynyas occurs in wind driven polynyas. Theoretical understanding of these polynyas is mainly based on so called polynya flux models, first introduced by Pease (1987). In terms of general circulation models polynyas must, however, be modelled using full scale dynamic-thermodynamic sea-ice models, not polynya flux models.

Bjornsson et al. (2001) compared the granular model of Tremblay and Mysak (1997) to the polynya flux model of Willmott et al. (1997) in an idealised basin. They found that the two models give very similar results. Here we expand on that work and compare the granular model to the more common viscous-plastic model of Hibler (1979) and the lesser known modified Coulombic yield curve by Hibler and Schulson (2000) in a similar setting Bjornsson et al. (2001) used.

We also consider the effects of initial and open boundary conditions as well as contrasting formulations by Hibler (1979) and Mellor and Kantha (1989) for the thickness of newly formed ice. Finally, we also examine the performance of the collection thickness parametrisation of Winsor and Björk (2000) to parametrise the new-ice thickness.

The layout of this paper is as follows: First the important points of the sea-ice model are outlined. In Sect. 3 we discuss the difference between polynya flux models and dynamic-thermodynamic models. The response of the granular model to the simple wind forcing is then considered, underlining the important features of polynya formation in the context of polynya flux models. Section 4 deals with the effects of initial and boundary conditions. In Sect. 5 the response of the model using different yield curves is discussed followed by a section discussing formulations for the thickness of newly

formed ice.

2 The model

The ice model is a fairly standard two class (ice and open water) dynamic-thermodynamic sea-ice model which was written to be coupled with the VOM ocean model (Backhaus, 2008). In the present context the most important points to discuss regarding the model are the facts that one can choose between three different viscous-plastic rheologies and two different ways in representing the newly formed ice. In this section we will briefly describe the model focusing on the rheology and new-ice thickness formulations.

The ice is modelled as a continuum using an Eulerian perspective. It moves in a horizontal plane, subject to both external and internal forces. Temporal evolution of the sea ice cover is described using two continuity equations and the momentum equation. The continuity equation for mass is simply

$$\frac{\partial m}{\partial t} + \nabla \cdot (\boldsymbol{v}\, m) = S_m\,, \tag{1}$$

where m is the total sea ice mass per cell, S_m is a thermodynamic source/sink term and $\boldsymbol{v}$ is velocity. An equation for the evolution of the ice thickness distribution within each cell is also needed. The model uses only two ice classes; i.e. ice and open water and so this becomes an equation of conservation of sea ice concentration. That takes the same basic form; i.e.

$$\frac{\partial A}{\partial t} + \nabla \cdot (\boldsymbol{v}\, A) = S_A\,, \tag{2}$$

with A denoting the fractional ice concentration per grid cell and S_A being the thermodynamic source/sink term. The average ice thickness over ice covered area, h can be derived using $m{=}Ah\rho_{\mathrm{i}}$ where ρ_{i} is a constant ice density. The thermodynamic terms, S_m and S_A will be discussed in Sect. 2.1.

In addition the condition $A \leq 1$ is imposed. This can be interpreted as a ridging condition since m (and thus h) can increase even if A does not. Together these equations describe the advection of the ice in a given velocity field.

The momentum equation used is (Coon et al., 1974)

$$\frac{\mathrm{D}(m\boldsymbol{v})}{\mathrm{D}t} = \tau_\mathrm{a} + \tau_\mathrm{w} - mf\boldsymbol{k}\times\boldsymbol{v} - mg\nabla H - \nabla\cdot\boldsymbol{\sigma}\,. \tag{3}$$

Here $\boldsymbol{k}$ is a unit vector normal to the surface, τ_a and τ_w are air and water stresses, f is the Coriolis factor, g is the gravitational acceleration, H is the sea surface height and $\boldsymbol{\sigma}$ is the sea ice stress tensor. Of the forcing terms on the right hand side $\nabla\cdot\boldsymbol{\sigma}$ describes forces due to internal stress while the other terms are all external factors. The material derivative on the left hand side is $\mathrm{D}/\mathrm{D}t = \partial/\partial t + \boldsymbol{v}\cdot\nabla$. The momentum equation is solved by repeatedly applying an SOR-solver, updating $\boldsymbol{v}$ and $\boldsymbol{\sigma}$ after each SOR-solve.

Wind and water stress are modelled as quadratic drag (McPhee, 1975);

$$\tau_\mathrm{a} = \rho_\mathrm{a} C_\mathrm{da} |\boldsymbol{v}_\mathrm{a}| \boldsymbol{v}_\mathrm{a} \tag{4}$$

$$\tau_\mathrm{w} = \rho_\mathrm{w} C_\mathrm{dw} |\boldsymbol{v} - \boldsymbol{v}_\mathrm{w}| (\boldsymbol{v} - \boldsymbol{v}_\mathrm{w}), \tag{5}$$

where C_dw and C_da are drag coefficients, ρ_w and ρ_a are air and water densities and $\boldsymbol{v}_\mathrm{w}$ and $\boldsymbol{v}_\mathrm{a}$ are the near surface water and wind velocities. We have assumed that the wind velocity is much larger than the ice velocity, i.e. that $|\boldsymbol{v} - \boldsymbol{v}_\mathrm{a}| \approx |\boldsymbol{v}_\mathrm{a}|$. The geostrophic turning angles used in McPhee (1975) have been set to zero since the near surface velocities are used, not geostrophic ones.

The representation of internal stresses in the model is done through the gradient of the stress tensor $\boldsymbol{\sigma}$. Stress and strain rate ($\dot{\boldsymbol{\varepsilon}}$) are related through the sea ice rheology and the three available rheologies will be discussed in Sect. 2.2.

2.1 Thermodynamics

The sea-ice model uses the three layer heat conduction scheme described in Semtner (1976), with the exception that surface fluxes are calculated using the relevant

equations in Idso and Jackson (1969) and Liu et al. (1979) and assuming a constant incoming short wave radiation flux. The ocean cooling is calculated using the thermodynamics routines from VOM (which are the same as in Harms et al., 2003). Our main interest here is, however, the formation of new ice over open water.

Ice formation in open water is modelled in a relatively simple fashion. When the temperature of the ocean surface falls below freezing new ice is formed. The amount of ice formed is calculated from the energy needed to bring the ocean surface from its super-cooled state to freezing, i.e.

$$Q_{\mathrm{ow}} = \rho_{\mathrm{w}} c_{\mathrm{w}} h_{\mathrm{w}} (T_{\mathrm{f}} - T_{\mathrm{w}}) \tag{6}$$

where c_{w} is the ocean heat capacity, h_{w} the mixed layer depth, T_{w} the ocean temperature and T_{f} the freezing point of sea water. The amount of ice formed in the open water is then

$$\Delta h_{\mathrm{ow}} = \frac{Q_{\mathrm{ow}}}{\rho_{\mathrm{i}} L_{\mathrm{i}}}, \tag{7}$$

where L_{i} and ρ_{i} are the latent heat of fusion and density for sea ice, respectively.

This, along with the changes in thickness of the ice already present in the grid cell now needs to be related to the continuity Eqs. (1) and (2) via the source/sink terms S_m and S_A. Deriving an equation for S_m is not difficult since it is a mass conservation formula. This term can be written out simply as

$$S_m = \rho_{\mathrm{i}} [A \Delta h + (1 - A) \Delta h_{\mathrm{ow}}], \tag{8}$$

where Δh represents thickness changes in the ice already present in the grid cell.

It is, however, not possible to derive an equation for S_A in such simple terms and the equation for it must be empirical or heuristic. Two common methods for calculating S_A are due to Hibler (1979) and Mellor and Kantha (1989). Hibler devised his method using fixed thermodynamic growth rates instead of calculating Δh and Δh_{ow}, but the method is easily adopted to our approach, giving

$$S_A = (1 - A) \max(\Delta h_{\mathrm{ow}}, 0) / h_0 + A \min(S_m, 0) / 2m, \tag{9}$$

where h_0 is a constant demarcation thickness separating thick and thin ice. Hibler (1979) assumed a constant h_0, but in Sects. 6 and 7 we discuss ways to parametrise it.

When freezing $\Delta h_{ow}>0$ and $S_m>0$ so Eq. (9) becomes simply

$$S_A h_0 = (1-A)\Delta h_{ow}. \tag{10}$$

This means, in particular that the new ice covers an area S_A so that its thickness is greater than or equal to h_0.

Another approach to calculating S_A is due to Mellor and Kantha (1989). They formulate S_A as

$$S_A = \Phi(1-A)\frac{Q_{ow}}{\rho_i L_i h}, \tag{11}$$

where Φ is an empirically determined function. Mellor and Kantha (1989) differentiate between melting and freezing by giving Φ different constant values;

$$\Phi = \begin{cases} \Phi_F = 4 & \text{if} \quad Q_{ow} > 0 \\ \Phi_M = 0.5 & \text{otherwise}. \end{cases} \tag{12}$$

We can easily recover Eq. (10) from Eq. (11) by setting $\Phi_F = h/h_0$, which gives $h_0 = h/\Phi_F$. Equation (11) therefore states that during freezing the newly formed ice will have a thickness equal to h/Φ_F. In particular, this means that when ice forms in a grid cell that had no ice before this cell will become fully covered with thin ice.

2.2 Rheology

The viscous-plastic rheologies discussed here describe isotropic ice and thus have a yield surface that is a curve in the stress invariant plane, i.e. $F(\sigma_I, \sigma_{II}, \text{scalars})=0$. The modelled stress states should lie close to the yield curve. For stresses inside or outside the yield curve viscous deformation occurs, while for stresses on the yield curve plastic deformation takes place.

In a viscous-plastic model the plastic and viscous behaviour can be represented using the stress invariants

$$\begin{aligned} \sigma_{\mathrm{I}} &= \zeta \dot{\varepsilon}_{\mathrm{I}} - P/2 \\ \sigma_{\mathrm{II}} &= \eta \dot{\varepsilon}_{\mathrm{II}}, \end{aligned} \tag{13}$$

where ζ and η are the non-linear bulk and shear viscosities and P is a pressure term. The strain rate invariants $\dot{\varepsilon}_{\mathrm{I}}$ and $\dot{\varepsilon}_{\mathrm{II}}$ are given by

$$\begin{aligned} \dot{\varepsilon}_{\mathrm{I}} &= \dot{\varepsilon}_{11} + \dot{\varepsilon}_{22} \\ \dot{\varepsilon}_{\mathrm{II}} &= \sqrt{(\dot{\varepsilon}_{11} - \dot{\varepsilon}_{22})^2 + 4\dot{\varepsilon}_{12}^2} \end{aligned} \tag{14}$$

where

$$\dot{\varepsilon}_{ij} = \frac{1}{2}\left(\frac{\partial v_i}{\partial x_j} + \frac{\partial v_j}{\partial x_i}\right). \tag{15}$$

In a viscous-plastic model the viscosities, ζ and η depend on $\dot{\varepsilon}$ and some scalars representing the ice state.

In Hibler's (1979) model the viscosities are functions of $\dot{\varepsilon}$ the ice pressure, P. They are then formulated such that the resulting yield curve is an ellipse and that for typical strain rates normal plastic flow applies. This yield curve reproduces basic sea ice characteristics, i.e. the ice is weak in tension, strong in shear and strongest in compression. It is at the same time mathematically very simple.

The viscosities are given by

$$\zeta = P/2\Delta \quad \text{and} \quad \eta = \zeta/e^2, \tag{16}$$

where P is the ice pressure,

$$\Delta = \sqrt{\dot{\varepsilon}_{\mathrm{I}}^2 + \dot{\varepsilon}_{\mathrm{II}}^2/e^2}, \tag{17}$$

e is the ratio of the ellipse axes.

It is clear that for small strain rates the viscosity tends to infinity so an upper bound must be set for ζ (and η). Hibler (1979) chose the limiting values to depend on the pressure term as

$$\begin{aligned} \zeta_{\max} &= (2.5 \times 10^8 \mathrm{s}) P, \\ \eta_{\max} &= \zeta_{\max} / e^2. \end{aligned} \tag{18}$$

In addition minimum values on ζ and η were imposed to improve numerical stability. Hibler (1979) chose

$$\begin{aligned} \zeta_{\min} &= 4 \times 10^8 \mathrm{kg/s} \\ \eta_{\min} &= \zeta_{\min} / e^2, \end{aligned} \tag{19}$$

arguing that this value is several orders of magnitude below typical strong ice interaction values, effectively yielding free drift results.

Finally the pressure term itself depends on the ice thickness and concentration. The form chosen by Hibler (1979) was

$$P = P^* h \exp(-C[1-A]), \tag{20}$$

where P^*, the ice strength and C are constants, h is the ice thickness and A the concentration. The constants must be chosen empirically, but $P^* \approx 30 \times 10^3$ N/m and C=20 are common choices (Hibler, 1979; Hibler and Walsh, 1982; Tremblay and Hakakian, 2006; Feltham, 2008). Hibler (1979) used e=2, which remains a popular choice. The ellipse in Fig. 1 depicts the Hibler (1979) yield curve.

A somewhat different approach to the elliptic yield curve was suggested by Tremblay and Mysak (1997), proposing a model based on a granular material rheology. For deformation along a sliding line, the following failure criterion (based on Coulomb's friction law) must be met:

$$\tau_s = -\sigma_s \tan\phi, \tag{21}$$

where ϕ is the macroscopic angle of friction and τ_s and σ_s are, respectively, the shear and normal stress acting on the sliding plane. This is equivalent to dynamic friction between two dry surfaces where the frictional force is proportional to the normal force. The constant of proportionality is the coefficient of friction $\tan\phi$. For stress ratios $-\sigma_s/\tau_s < \tan\phi$ the ice behaves like an elastic solid and for $-\sigma_s/\tau_s = \tan\phi$ it flows like a fluid. Equation (21) can also be written in terms of the two stress invariants, σ_I and σ_{II};

$$\sigma_{II} = \sigma_I \sin\phi. \tag{22}$$

The resulting constitutive law has the same form as the constitutive law in Eq. (13), but with $\zeta=0$ and $-P\delta_{ij}/2$ replaced with $-P\delta_{ij}$. The value of η, which here should be referred to as the coefficient of friction, is given by

$$\eta = \frac{P\sin\phi}{\dot{\varepsilon}_{II}}. \tag{23}$$

The ice pressure $P=-\sigma_I$ is then found by fulfilling the equation

$$\dot{\varepsilon}_I = \dot{\varepsilon}_{II}\tan\delta, \tag{24}$$

where δ is the angle of dilatency. The pressure is therefore only related to ice thickness and concentration through the upper limit set on it;

$$P_{max} = P^* h \exp(C[1-A]), \tag{25}$$

analogously to Eq. (20). To facilitate comparison with the other two model formulations P_{max} is scaled with $(1+\sqrt{1+1/e^2})/(2[1+\sin\phi])$ (Tremblay and Hakakian, 2006). The pressure is calculated using an iterative solver which means that the numerical performance of the granular model is considerably worse than that of Hibler's model.

Since $\zeta=0$ the granular material rheology has the form of an incompressible Newtonian fluid with non-linear shear viscosity. Compressibility is, however, present in the model since the pressure term has a maximum value of P_{max}. For small strain rate

values the coefficient of friction, η, must also be set to a constant value $\eta_{\max}$ resulting in a viscous behaviour of the ice under those conditions. The resulting yield curve is a triangle (see Fig. 1), which is realistic for small strain rates, but may not be very realistic for large strain rates.

Finally we discuss a model formulation which can be thought of as a combination of the other two. This formulation uses the so-called modified Coulomb yield curve, first set forward by Hibler and Schulson (2000) when studying anisotropic approaches to sea ice modelling, but later used in a large scale, isotropic model by Heil and Hibler (2002). The curve gives friction-based failure up to a limiting compressive stress while for higher stresses ridging occurs. This limit is set at pure shear deformation, in accordance with the results of laboratory experiments. The yield curve also includes a small amount of tensile stress. The resulting shape is similar to the ice cream cone suggested by Coon et al. (1974) and should be fairly realistic for all strain rates (see Fig. 1).

The modified Coulombic yield curve is probably best described by first considering an elliptic yield curve as described earlier. Now demand that for low stress the yield curve be Coulombic, not elliptic. Hibler and Schulson (2000) achieve this by setting

$$\eta = \min(\zeta/e^2, \eta_1), \tag{26}$$

where

$$\eta_1 = \frac{P/\alpha - 2\zeta\dot{\varepsilon}_{\mathrm{I}}}{\beta\dot{\varepsilon}_{\mathrm{II}}}, \tag{27}$$

with α=1.8 and β=1.4. In addition they use a smaller axes ratio of $e=\sqrt{1.91716}$. This gives the desired Coulombic shape for low stress. Additionally, to ensure that there is no stress at zero strain rates Hibler and Schulson (2000) set

$$P' = 2\gamma\Delta\zeta, \tag{28}$$

with γ=0.91 and replace P with P' in Eq. (13).

There are no lower bounds for the values of ζ and η, unlike in the elliptic formulation, and the upper bound used is considerably lower, $\zeta_{max}=10^6$ kg/s instead of $\zeta_{max}=4\times10^8$ kg/s, used for the ellipse.

3 Basic model characteristics

The model used in this study is a dynamic-thermodynamic sea-ice model in a set-up similar to what Bjornsson et al. (2001) used. In this section we will discuss wind-driven polynyas and compare dynamic-thermodynamic models to polynya flux models in order to better understand the limits of the former model type. We will then discuss the important characteristics of our model set-up.

Wind-driven coastal polynyas are conceptually relatively simple. They form where the ocean is initially covered by ice and a wind starts blowing off the coast. This then causes the ice to move off-shore opening up a polynya at the coast (or fast ice edge). Inside the polynya the ocean is at the freezing point and so frazil ice forms, which is herded down stream by the wind and waves. This frazil ice then consolidates at the edge of the initial ice. The polynya remains open as long as the off-shore component of the wind remains strong enough to keep it open.

Polynya flux models are based on assumptions about the ice formation rate and the velocity of the ice. The first polynya flux model was developed by Pease (1987), which proposed a simple one-dimensional time-dependent model. Several improvements and extensions have been made to this model, most notably those by Ou (1988); Willmott et al. (1997) and Biggs et al. (2000).

In Pease's model one assumes that the initial ice pack drifts away from the shore at a constant speed. The frazil ice formed in the polynya is immediately transferred from inside the polynya to the edge of the initial ice pack. There the frazil consolidates into new ice of a given thickness, referred to as the collection depth (H). The polynya edge is then at the edge of this consolidated ice and the edge position is balanced between the ice formation rate and the drift speed of the consolidated ice (and the initial ice

pack). As time passes the initial ice pack drifts away and is replaced by consolidated ice (see upper panel of Fig. 2).

The Pease (1987) model therefore stipulates three distinct ice regimes in a polynya simulation: The thick initial ice, the consolidate ice and the polynya itself. In the Pease (1987) model no ice is found inside the polynya, but in general frazil ice or ice of other ice types may be found inside the polynya, at a low concentration. The polynya edge is the interface between the polynya and the consolidated ice. Polynya flux models assume the polynya edge is both well defined and sharp.

Ou (1988) improved the model by Pease (1987) by assuming the frazil ice travels at a finite speed from inside the polynya towards the polynya edge. Willmott et al. (1997) extended this model to two dimensions. The Ou (1988) model still assumes the frazil ice drifts faster than the consolidated ice so the fast moving frazil crystals pile up against the slower consolidated ice.

In reality the frazil drifts faster than the consolidated ice because frazil ice, near or at the surface, experiences less water shear stress than the consolidated ice. The water velocity inside the polynya is also different from that under the consolidated ice, but this can be very difficult to account for in a simplified set-up. Finally the initial ice pack may also not drift at the (local) free drift speed as the wind that creates the polynya is non-uniform and may be weaker further off shore. Islands and other coast lines may also slow down the drift of the initial ice pack.

An important point in improving the Pease (1987) model has been to replace the constant collection depth with some parametrisation. Winsor and Björk (2000) parametrised the collection depth based on wind speed, but their parametrisation is not necessarily compatible with the Ou (1988) model. Biggs et al. (2000) introduced a different parametrisation for H for the Ou (1988) model, taking into account the different velocities for frazil and consolidated ice. The parametrisation of Biggs et al. (2000) has been improved upon since then, most recently by Walkington et al. (2007).

The main drawback of using polynya flux models is that they cannot easily be coupled with general circulation ocean and atmosphere models. The dynamic-thermodynamic

sea-ice models, such as the one used here, are on the other hand designed for such a coupling and to model sea-ice in general, not only polynyas.

While quite sufficient for modelling pack ice, dynamic-thermodynamic sea-ice models generally don't include any frazil ice parametrisations. When ice forms over open water a block of solid ice of a predetermined thickness, h_0 (see Sect. 2.1), is immediately formed, akin to pancake ice. When ice is already present in the grid cell one could argue that frazil ice is produced and then immediately "piles up" against the pancake ice – similar to what happens in the Pease (1987) model.

In a polynya the pancakes drift towards the initial ice pack forming the consolidated ice, which consequently has thickness h_0. Figure 2 shows a diagram comparing ice formation in polynya flux models and dynamic-thermodynamic models. As the figure shows, we expect the dynamic-thermodynamic model also to show the three ice regimes the flux polynya models do. Additionally we expect a sharp polynya edge and higher ice velocity inside the polynya than in the consolidated and thick ice. Based on the results of Bjornsson et al. (2001) we can also expect the different rheological formulations of the dynamic-thermodynamic model to give polynyas of similar size and shape as the granular model.

A polynya modelled by a dynamic-thermodynamic model therefore contains no frazil ice, only pancake ice, which is unrealistic. This may affect the modelled oceanic heat loss since the pancake ice is a more effective insulator than the frazil ice. In order to ensure reasonably large oceanic heat loss inside the polynya it is important that the ice concentration there remains sufficiently low. To that end Bjornsson et al. (2001) chose h_0=30 cm, even though pancake ice is usually somewhat thinner or around 10 cm thick.

Modelling the frazil ice as pancakes also has its drawbacks when considering the ice dynamics. If the ice concentration is not too high ($A \lesssim 0.8$ for the model formulations and parametrisations used here) both the pancake and consolidated ice are in free drift. The problem is that the free drift speed of these two are the same. This means that if the initial ice pack drifts away from the coast at free drift the polynya that opens up fills with pancake ice drifting at the same speed. Instead of a sharp polynya edge this

set-up will result in linearly increasing ice concentration inside the polynya. In reality the frazil ice inside the polynya drifts faster than the consolidated ice causing a polynya edge to form.

Bjornsson et al. (2001) noted this behaviour (see their Fig. 4). In their study a polynya edge forms because the drift of the consolidated ice is slowed down by one of the side walls of their ideal basin. This approach is also used here.

Our set-up consist of a bay, 135 by 75 km, which is initially covered by thick ice. A polynya is then created by having a 20 m/s wind blow uniformly at a 30° angle to the direction along the bay, as shown in Fig. 3. This way the ice will drift out of the bay, but will also pile up on the down-wind side of the bay, slowing down its drift. This creates a difference between free drift velocity and the velocity of the consolidated ice which is necessary for the formation of a polynya edge.

The atmospheric temperature is kept constant at $T_{air}=-20°C$ and the oceanic temperature is kept at the freezing point for a salinity of $S=32$. The water velocity is always zero. Unless stated otherwise, the model is initialised with ice concentration $A=0.9$ and thickness $h=1$ m. For the solid boundaries, a no-slip condition is used while for the open boundary zero gradient von Neumann boundary conditions are applied to all variables, except the ice pressure P which is set to zero in accordance with Bjornsson et al. (2001) and Dukowicz (1997). A list of the relevant constants is included in Table 1.

The granular model is expected to give reasonably good results for the current set-up, based on the study by Bjornsson et al. (2001). We will therefore use it to investigate attributes of the polynya not related to the rheology itself.

To illustrate the temporal evolution of the polynya Fig. 4 shows a Hovmöller diagram of the ice concentration field taken along a section at $y=37.5$ km. The response to the applied wind stress is immediate and a discernible polynya edge starts to form during the first day of the model integration. After two days the polynya has a clear structure and can be considered fully formed. A practically steady state has been reached after eight days. After the polynya has fully formed there always exists a band of large gradient in the concentration field representing the polynya edge. For further reference

Fig. 5 shows the ice concentration in the basin after eight days of model integration. As Figs. 4 and 5 show, the edge in this simulation is at a concentration of between A=0.7 and A=0.9.

Ice formation rates in the model are closely linked to the fractional ice concentration. For open water the ice formation rate is $F(A{=}0){\approx}27$ cm/day, while for A=1 and h=30 cm the ice formation rate is $F(A{=}1){\approx}6$ cm/day. The thickness of the pancake ice only increases very slightly and so nearly all the ice growth contributes to increasing the ice concentration. This means that the ice formation rate for $A \in]0,1[$ can be approximated by a weighted average of $F(A{=}0)$ and $F(A{=}1)$. Defining the polynya as all points for which A<0.8, the mean ice formation rate in the polynya is F=14.1 cm/day after two days and F=13.2 cm/day after 8 days.

According to Ou (1988) ice velocity in the model should fall into two categories; that of free drift in the polynya itself and that of the consolidated ice. In the dynamic-thermodynamic model this velocity change gives the pancake ice drifting in the polynya a barrier of slower consolidated ice to pile up against. Figure 6 shows the velocity field and speed in the control experiment after eight days. The speed does indeed fall into two categories with the free drift speed $|\boldsymbol{v}_f|$=32.6 cm/s and the speed of the consolidated ice $|\boldsymbol{v}_c| \lesssim 30$ cm/s, depending on the distance away from the y=75 km boundary. In the polynya the pancake ice drifts with the wind but the consolidated ice slides along the y=75 km boundary with a small cross channel velocity component due to ridging at the boundary. Near the open boundary the ice velocity increases rapidly because the ice pressure P is set to zero.

4 Initial and boundary conditions

When studying a system of differential equations the initial and boundary conditions are usually worthy of some consideration. Given the simplistic set-up used here the initial and boundary conditions are also as simple as possible. In this section we will, however, consider two cases which may not be immediately obvious; that of varying initial

TCD
3, 1023–1068, 2009

ice thickness and of different treatment of the ice pressure P on the open boundary.

The initial ice thickness dictates the ice strength as the polynya starts forming. Figure 7 shows the polynya edge after two days using initial ice thickness of 30 cm, 60 cm and 2 m. The thicker ice is naturally stronger, both in shear and compression. Differences in compressive strength are seen as a shift along the y-axis while differences in shear strength show as a shift along the x-axis. The ice yields to compression through ridging which only occurs at the y=75 km boundary.

The polynya thus opens up faster when the ice is thinner, but the difference is largest after about two days. As the initial ice flows out of the domain its influence decreases and, in particular, the final steady state is independent of the initial thickness.

The open boundaries have limited effects on the polynya edge and formation. This can be shown by running the model in a longer bay and noting that all main results are unchanged. Another approach is to extend the zero gradient condition to the ice pressure, P, as well. Using P=0 at the open boundary assumes the ice can flow freely out of the domain, but assuming $\partial P/\partial x$=0 assumes that the ice just outside the boundary has the same strength as the ice just inside the boundary. This should, in essence be equivalent to using an infinitely long homogeneous channel.

There are a few features associated with the open boundaries, but these effects are only noticeable near the open boundary and don't affect the interior of the domain. Ice velocity is the most sensitive to the open boundary and Fig. 8 shows the speed and velocity after eight days using the von Neumann condition. It should be compared to Fig. 6 which shows speed and velocity using P=0 at the open boundary. Although there are marked differences in the velocities between the two boundary conditions, such large differences are not seen in the other results.

Using a channel twice as long as the one used in the control run gives results nearly identical to those using the von Neumann condition, in the region common to both setups. The von Neumann condition therefore simulates well the situation where there is large amount of ice just outside the open boundary. Using P=0 on the other hand assumes very little ice just outside the open boundary. We note also that the von

Neumann condition fulfils the stability criterion set forward by Dukowicz (1997) and works equally well using the other rheologies.

5 Different yield curves

An important part of the motivation for this study was to compare the results of Bjornsson et al. (2001), using the granular model, to a similar set-up using different rheologies. In this section we consider the response of the elliptic yield curve, proposed by Hibler (1979) and that of the modified Coulombic yield curve from Hibler and Schulson (2000). This focuses on the model response in the region of the initial ice pack and that of the consolidated ice, since the rheology should not play a role inside the polynya itself.

The viscous-plastic formulation with an elliptic yield curve proposed by Hibler (1979) is by far the most popular rheology in use today in dynamic-thermodynamic sea-ice models. Both it and the modified Coulombic yield curve are also numerically more efficient than the granular model.

Using the Hibler (1979) formulation unmodified, however, does not meet our expectations of the model performance, as stated in Sect. 3. The polynya structure is very diffuse with no clear polynya edge, as Fig. 9 shows. Speed and velocity, in particular, fail to meet the criteria for forming a polynya edge; i.e. there is no clear separation between the velocity of pancake ice and consolidated ice. In addition, the consolidated ice flows faster than the pancake ice, which is clearly unrealistic.

On closer inspection one can see that this result is due to the fact that the model responds mostly in a linear viscous way. In his original formulation Hibler (1979) used a minimum on ζ as $\zeta_{\min}=4.0\times10^8$ kg/s "in order to insure against any non-linear instabilities" noting that that value is "several orders of magnitude below typical strong ice interaction values and effectively yields free drift results" (Hibler, 1979). Later papers by Hibler usually don't mention this cap (see for instance Lepparanta and Hibler, 1985) and many ice modellers don't use it. All in all, it has received little attention in the

literature.

In the current set-up, the viscosity parameter ζ is consistently kept at its minimum value for $A \lesssim 0.9$ throughout the simulation. This is because the viscosity is related to the ice pressure via Eq. (16) and the pressure to ice concentration via Eq. (20). The flow where A is sufficiently small is therefore linear viscous, but choosing as a minimum $\zeta_{\min}=4.0\times10^{8}$ kg/s does not result in effectively free drift, at least not for such a high resolution.

Running the model with $\zeta_{\min}=0$ kg/s alleviates all these problems and the results are then practically identical to those obtained using the granular model. Using $\zeta_{\min}=0$ kg/s we observerd no non-linear instabilities. Another approach would be to choose a low, but non-zero value for $\zeta_{\min}$. The resolution of Hibler's model was 125 km and since viscosity scales with the distance squared a choice of $\zeta_{\min}=4\times10^{4}$ kg/s seems in order. This yields nearly the same results as with $\zeta_{\min}=0$ kg/s; the largest difference in concentration between the two model runs being $\Delta A=0.004$.

Unfortunately perhaps the computing cost is also almost the same and since we experience no instabilities in our model nothing much appears to be gained from choosing a small non-zero value for $\zeta_{\min}$ over choosing $\zeta_{\min}=0$ kg/s. When choosing even larger values the effects of capping ζ also start to show. For $\zeta_{\min}=4\times10^{5}$ kg/s the difference between that run and the one with zero $\zeta_{\min}$ is $\Delta A=0.02$ and for $\zeta_{\min}=4\times10^{6}$ kg/s the difference is $\Delta A=0.2$.

Using the modified Coulombic yield curve also gives results very similar to the granular model. This is to be expected, since the modified Coulombic yield curve is in a way a combination of the other two yield curves. Figure 10 shows the polynya edge, defined by $A=0.8$ using each of the three rheologies after eight model days. The difference between the three model formulations is only marginal, but the polynya is slightly larger when using the granular model.

6 New-ice thickness

As we've already seen the ice rheology affects the initial ice pack and the consolidated ice. The inside of the polynya, on the other hand, is mostly affected by the new-ice thickness parametrisation. This determines the thickness, and thus the concentration of the ice formed inside the polynya.

The most popular method for parametrising the new-ice thickness is probably the one suggested by Hibler (1979) (see Sect. 2.1). Put simply the new-ice thickness is not allowed to drop below a certain minimum, h_0. If the total mass of newly formed ice is not enough to cover the open water fraction of the grid cell at that thickness then the concentration of newly formed ice is adjusted accordingly. If more ice is formed then the new ice is simply thicker than h_0.

The choice of h_0 is not obvious and appears to range from 10 to 50 cm or even more in some cases. Bjornsson et al. (2001) argued for using h_0=30 cm and that is the value used here so far. Their argument is based on the assumption that the ice that forms in the polynya immediately forms pancake ice. However, 30 cm is quite thick for pancake ice which is closer to being 10 cm thick, as they point out as well. It is therefore worth considering a model run with h_0=10 cm.

The main result of this run is that with a lower h_0 the polynya fills up much faster. The newly formed ice is thinner, has therefore larger surface area, resulting in higher ice concentration in the polynya itself and causes the polynya edge to form closer to the bottom of the bay than before. This can be seen in Fig. 11 which shows the fractional ice concentration using h_0=10 cm after eight days.

Higher ice concentration also leads to lower ice formation rates in the polynya; the average ice formation rate in the polynya is F=11.3 cm/day after two days and F=11.0 cm/day after 8 days. This is about 20% lower than in the control run. This is due to the fact that majority of the ice formation occurs over open water. Finally the consolidated ice is naturally thinner as well since its thickness equals h_0.

The other approach to determining the thickness of newly formed ice described in

Sect. 2.1 is the one due to Mellor and Kantha (1989). There the thickness of newly formed ice is based on the thickness of the ice already present in the grid cell. Mellor and Kantha (1989) argued that the thickness of newly formed ice should be a quarter of the old ice thickness. This means also that when there is no ice in the grid cell when new ice forms the ice is uniformly spread over the entire cell, potentially very thinly. A polynya in such a model may therefore be hard to recognise by the change in concentration and researchers using this approach often consider ice below a certain cut-off thickness to represent the polynya. Smedsrud et al. (2006), for instance, use 30 cm for this cut-off thickness, which, in light of our previous discussion sounds reasonable.

As expected, using this approach results in a "polynya" that is hardly recognisable in the concentration field, as Fig. 12 shows. Even after eight days there is only a thin sliver of an opening along the x=0 km and y=0 km boundaries and the A=0.9 isoline is at most only 10 km away from the shore. More seriously perhaps the velocity field, also shown in Fig. 12, shows no signs of the discontinuity deemed necessary for proper polynya formation. The ice where A<0.9 does indeed flow with the same free drift speed as before, but when it reaches the "edge" it slows down very gradually, contrary to our previous assumptions about how a polynya is formed.

The ice thickness near the coast is indeed lower than the initial ice thickness, but as Fig. 13 shows there is no real polynya edge to be found in the ice thickness. As before the thick initial ice drifts out of the basin, but in this case the ice that replaces it does not have a uniform thickness. It is very thin at the coast with linearly increasing thickness towards the thick initial ice.

We have already mentioned that considerable effort has been put into parametrising the collection thickness in polynya flux models. Given the large variation between the results already presented in this section we find it worth considering if the polynya flux model parametrisations can be applied in the dynamic-thermodynamic model.

The parametrisation by Winsor and Björk (2000) lends itself well to immediate inclusion in the dynamic-thermodynamic model. It's based only on the wind speed and not

the polynya width, frazil ice speed or other quantities not accessible to the dynamic-thermodynamic model.

Using the Winsor and Björk (2000) parametrisation the ice behaviour inside the polynya is therefore still rather unrealistic, but the consolidated ice thickness and thus the size of the polynya should be more realistic.

Winsor and Björk (2000) assumed the collection depth changed as

$$H = \frac{1 + 0.1|\boldsymbol{v}_a|}{15}, \tag{29}$$

where $|v_a|$ is the surface wind velocity. In particular, $H \approx 7$ cm for $|v_a|=0$ and $H=30$ cm for $|v_a|=35$ m/s so this parametrisation is well within the range of plausible values for h_0. Equation (29) is then used to calculate h_0 in each grid point.

Using this parametrisation results in smaller polynyas at low wind speeds, compared to $h_0=30$ cm or larger polynyas at high wind speeds, compared to $h_0=10$ cm. Figure 14 shows that the difference can be quite considerable for the wind speed range of [10,30] m/s. At lower winds the polynya edge starts to become diffuse, which is to be expected.

Ice formation rate (F) using Eq. (29) also lies between the $h_0=10$ cm and $h_0=30$ cm values (see Fig. 15). Still, we note that the ice formation rate using the parametrisation is always fairly close to that when using $h_0=30$ cm and grows steadily with increasing wind strength. Using this parametrisation therefore gives us the large ice-formation rates Bjornsson et al. (2001) were aiming for by using a large h_0.

7 Discussion

Bjornsson et al. (2001) have already shown that the granular model can be used to model polynyas in an idealised setting with quite acceptable results compared to a polynya flux model. We have shown that this is also the case when using the modified Coulombic yield curve of Hibler and Schulson (2000) and when using the elliptic

yield curve of Hibler (1979) with ζ_{min} sufficiently small. This is important since the numerical performance of the granular model is considerably worse than that of the other two models.

Using a large ζ_{min}, in particular $\zeta_{min}=4\times10^8$ kg/s which Hibler (1979) suggests does, however, give very unrealistic results. Using this original formulation gives a polynya which is smeared out with no proper edge and a velocity field which has little relation to polynya formation. This happens because the capping of ζ in the model turns the viscous-plastic formulation into a linear viscous model for ice concentration $A<0.9$. Using the elliptic yield curve with a capped ζ is therefore not a good way to simulate polynyas. Removing the cap is easy enough and this results in a model which is much better capable to model polynyas in a high resolution.

Although not investigated here, these considerations should equally apply to models of the marginal ice zone. There the concentration and thickness is often low so using a capped ζ may result in linear viscous behaviour as it does in the polynya simulation. This would then cause the marginal ice zone to be too diffused with little structure to it and should as well cause it to respond incorrectly to applied forcing.

With the exception of a capped ζ, all three yield curves give nearly identical results. Looking at the stress states we see that using the granular model the σ_I values are nearly all clustered around P_{max}. This means that at nearly all model points the ice cover is yielding or very close to yielding under compression. Bjornsson et al. (2001), on the other hand, have shown that the ice strength parameter P^* has little influence on the model results and so we can assume that while the ice cover does compress somewhat then it is so slight as to be inconsequential. It then becomes clear that the behaviour of the ice cover is largely controlled by Eq. (25), which is also one of the main equations governing the behaviour of the other two yield curves. The difference between the granular model and the other two, seen in Fig. 10 is then almost entirely explained by the different formulation of shear strength between the model formulations. As the figure shows the granular model gives slightly lower shear strength.

The stress states using the other two yield curves are much more evenly distributed

TCD
3, 1023–1068, 2009

along the σ_1 axis. For the modified Coulombic yield curve the stress states that lie on the Coulombic slope are all inside the polynya while the stress states in the consolidated ice are all on the elliptic part of the yield curve. This happens because in the consolidated ice compressive strain is always positive so according to Eq. (13) $\sigma_1 \leq -P/2$. Using the elliptic and modified Coulombic yield curves therefore yields similar results for the consolidated ice, where both yield curves have an elliptic shape. The pancake ice is in free drift so the shape of the yield curve has no effect there.

A final point in the dynamic considerations here is the fact that the ice behaviour at the open boundary can be described very well using von Neumann boundary conditions on all variables, including P. Bjornsson et al. (2001) set $P=0$ at the open boundary, which increases the ice velocity there in an unrealistic manner. This is a common practice when dealing with open boundaries and is reasonable when one expects little ice outside the domain. Using $\partial P/\partial x=0$ (or $\nabla P=0$) at the open boundary is, however, feasible when one expects similar amounts of ice inside and outside the open boundary.

In terms of thermodynamics we considered three ways in which to parametrise the thickness of ice forming over open water. These are the methods suggested by Hibler (1979), Mellor and Kantha (1989) and an adaptation of the collection thickness parametrisation by Winsor and Björk (2000). Hibler's method was used when investigating the dynamic aspects (Sects. 2–5) with an ice demarcation thickness $h_0=30$ cm after Bjornsson et al. (2001). That value may be somewhat high and so we also ran the model using $h_0=10$ cm.

This resulted in a smaller polynya with higher ice concentration and lower ice formation rates. In other respects the behaviour of the model remained the same; a sharp polynya edge separated the consolidated ice and pancake ice and the velocity field showed a nice discontinuity at the polynya edge. The width of the polynya did decrease, but that was to be expected and can also be understood in relation to the

Lebedev-Pease width of a polynya (Pease, 1987)

$$L = \frac{HU}{F}, \tag{30}$$

where L is the polynya width and HU is the flux of consolidated ice. An in-depth comparison with a polynya flux model was therefore not deemed necessary at this point.

Results obtained using the formulation of Mellor and Kantha (1989) were, however, vastly different from those obtained in the control run. Using Mellor and Kantha's formulation there are two ice regimes; thick ice and thin ice, which may be characterised as nilas. This replaces the threefold separation of thick ice, consolidated ice (of uniform thickness) and frazil/pancake ice, seen in flux polynya models and the control run. The polynya edge is considered to be what separates the consolidated ice and frazil/pancake ice, but this distinction is lost when using the Mellor and Kantha (1989) approach. The new-ice thickness formulation by Mellor and Kantha (1989) is therefore not suitable for modelling polynyas.

One could argue that the sharp edge separating frazil and consolidated ice in polynya flux models is not realistic (see for instance Smedsrud and Skogseth, 2006). This is important to us here since the fact that Mellor and Kantha's approach gives poor representation of polynyas in part hinges upon this point. However, even though the edge of a polynya may not be accurately defined on the scale of metres or even hundreds of metres, the edge should all the same be fairly easy to define when the resolution is on the order of kilometres. We therefore feel quite comfortable demanding that our model give a sharp polynya edge, both in the concentration and velocity fields.

On the whole the approach in Hibler (1979) is also more reasonable. This is mainly because wind and waves, which cannot be resolved by ocean or atmosphere models, will transform the frazil ice in the polynya into pancake ice like that scheme assumes. The thin ice formed using Mellor and Kantha's approach is more akin to grease ice or nilas which form in calmer conditions.

Wind speed is therefore an important factor in determining the new-ice thickness and

it is consequently an important part of collection depth parametrisations for polynya flux models. Winsor and Björk (2000) parametrised the collection depth in the Pease (1987) model based only on wind speed and we found that parametrisation well suited for inclusion in the dynamic-thermodynamic model.

Using the Winsor and Björk (2000) parametrisation gives results in the range between the results when using a constant h_0 between 10 and 30 cm. We have already expressed a preference for the Hibler (1979) parametrisation and using the Winsor and Björk (2000) parametrisation enables us to choose a sensible value for h_0.

On a more general note such a small value for h_0 may not be suitable for models describing the central pack ice as well. In such a situation the approach of Mellor and Kantha (1989) may give better results since the thick pack ice appears to require a larger h_0.

It is trivial to combine all three approaches to new-ice thickness parametrisation discussed here into one:

$$h_0 = \max\left(\frac{h}{\Phi}, \frac{1+0.1|\boldsymbol{v}_a|}{15}\right), \tag{31}$$

with Φ=4. This approach modifies the previously constant h_0 of Hibler (1979) so that for thick ice the approach of Mellor and Kantha (1989) is used and for thinner ice the parametrisation of Winsor and Björk (2000) is used.

8 Conclusions

We have used an idealised set-up to test three different sea-ice rheologies and three different formulations for the thickness of newly formed ice during polynya formation. These tests were done using a dynamic-thermodynamic sea-ice model in an idealised channel, similar to what Bjornsson et al. (2001) did.

We were able to reproduce the results of the granular model using both the modified Coulombic yield curve of Hibler and Schulson (2000) and the elliptic yield curve of

Hibler (1979). This is important since the numerical performance of the granular model is substantially worse than that of the other two models.

We note, however, that using the elliptic yield curve gave unrealistic results when using too high minimum bulk viscosity $\zeta_{\min}$. The elliptic yield curve can be and often is used with $\zeta_{\min}$=0, but the role of $\zeta_{\min}$ appears not to have received much discussion in the literature. These results may also be relevant to other topics in sea-ice modelling, most probably modelling of the marginal ice zone.

We also suggested using a von Neumann condition on the ice pressure at the open boundary to better simulate the ice behaviour there. This proved to give nearly identical results to using a longer channel. We conclude that using the von Neumann condition is a viable option when one expects large amounts of ice joust outside the open boundary. Using P=0 on the other hand assumes very little ice just outside the open boundary.

The formulation of new-ice thickness suggested by Hibler (1979) turned out to give much better results than the one from Mellor and Kantha (1989). Using Mellor and Kantha's formulation failed to give a clear polynya edge, both in the concentration and velocity field. We conclude therefore that this approach does not enable us to properly model polynyas. Hibler's approach on the other hand gave a clear edge consistent with our understanding of polynyas based on polynya flux models.

Hibler (1979) assumed a constant demarcation thickness (h_0). We suggest, however, using the collection thickness parametrisation of Winsor and Björk (2000) to parametrise h_0. This results in a value for h_0 which is dependent on wind strength and in the range already deemed acceptable for h_0. As an aside a combination of this parametrisation with the approach of Mellor and Kantha (1989) is proposed. This should give a parametrisation for h_0 applicable for both the marginal ice zone and the central ice pack.

Acknowledgements. We would like to thank Dirk Notz for his thorough reading of the manuscript and helpful suggestions and Bruno Tremblay for useful discussions during the course of this work. We would also like to thank Stefan Heitmann for his help during the development of the ice model. This work was financed by the DFG under HA 3166/2-1 "STARBUG".

References

Backhaus, J.: Improved representation of topographic effects by a vertical adaptive grid in vector-ocean-model (VOM). Part I: Generation of adaptive grids, Ocean Model., 22, 114–127, doi:10.1016/j.ocemod.2008.02.003, 2008. 1026

Biggs, N. R. T., Morales Maqueda, M. A., and Willmott, A. J.: Polynya flux model solutions incorporating a parameterization for the collection thickness of consolidated new ice, J. Fluid Mech., 408, 179–204, doi:10.1017/S0022112099007673, 2000. 1034, 1035

Bjornsson, H., Willmott, A. J., Mysak, L. A., and Morales Maqueda, M. A.: Polynyas in a high-resolution dynamic-thermodynamic sea ice model and their parameterization using flux models, Tellus, 53A, 245–265, doi:10.1034/j.1600-0870.2001.00113.x, 2001. 1024, 1025, 1034, 1036, 1037, 1040, 1042, 1044, 1045, 1046, 1048

Coon, M. D., Maykut, G. A., Pritchard, R. S., Rothrock, D. A., and Thorndike, A. S.: Modeling the pack ice as an elastic-plastic material, AIDJEX Bull., 24, 1–105, 1974. 1027, 1033

Dukowicz, J.: Comments on "Stability of the viscous-plastic sea ice rheology", J. Phys. Oceanogr., 27, 480–481, doi:10.1034/j.1600-0870.2001.00113.x, 1997. 1037, 1040

Feltham, D. L.: Sea Ice Rheology, Annu. Rev. Fluid Mech., 40, 91–112, doi:10.1146/annurev.fluid.40.111406.102151, 2008. 1031

Harms, I., Hübner, U., Backhaus, J. O., Kulakov, M., Stanovoy, V., Stepanets, O., Kodina, L., and Schiltzer, R.: Siberian River Runoff in the Kara Sea: Characterization, Quantification, Variability and Environmental Significance, Chap. Salt intrusions in Siberian river estuaries: Observations and model experiments in Ob and Yenisei, 27–46, No. 6 in Proceedings in Marine Science, Elsevier, 2003. 1028

Heil, P. and Hibler III, W. D.: Modelling the high-frequency components of Arctic Sea ice drift and deformation, J. Phys. Oceanogr., 32, 3039–3057, doi:10.1175/1520-0485(2002)032<3039:MTHFCO>2.0.CO;2, 2002. 1033

Hibler, III, W. D.: A dynamic thermodynamic sea ice model, J. Phys. Oceanogr., 9, doi:10.1175/1520-0485(1979)009<0815:ADTSIM>2.0.CO;2, 1979. 1024, 1025, 1028, 1029, 1030, 1031, 1040, 1042, 1045, 1046, 1047, 1048, 1049

Hibler III, W. D. and Schulson, E. M.: On modeling the anisotropic failure and flow of flawed sea ice, J. Geophys. Res., 105, 17105–17120, doi:10.1029/2000JC900045, 2000. 1024, 1025, 1033, 1040, 1044, 1048

Hibler III, W. D. and Walsh, J. E.: On modeling seasonal and interannual fluc-

tuations of arctic sea ice, J. Phys. Oceanogr., 12, 1514–1523, doi:10.1175/1520-0485(1982)012<1514:OMSAIF>2.0.CO;2, 1982. 1031
Idso, S. B. and Jackson, R. D.: Thermal radiation from the atmosphere, J. Geophys. Res., 74, 5397–5403, doi:10.1029/JC074i023p05397, 1969. 1028
Lepparanta, M. and Hibler III, W.: The role of plastic ice interaction in marginal ice-zone dynamics, J. Geophys. Res., 90, 1899–1909, doi:10.1029/JC090iC06p11899, 1985. 1040
Liu, W. T., Katsaros, K. B., and Businger, J. A.: Bulk parameterization of air-sea exchange of heat and water vapor including the molecular constraints at the interface, J. Atmos. Sci., 36, 1722–1735, doi:10.1175/1520-0469(1979)036<1722:BPOASE>2.0.CO;2, 1979. 1028
Maykut, G. and Perovich, D.: The role of shortwave radiation in the summer decay of a sea ice cover, J. Geophys. Res., 92, 7032–7044, doi:10.1029/JC092iC07p07032, 1987. 1025
Maykut, G. A.: Large-scale heat exchange and ice production in the central Arctic, J. Geophys. Res., 87, 7971–7984, doi:10.1029/JC087iC10p07971, 1982. 1024
Maykut, G. A. and McPhee, M. G.: Solar heating of the Arctic mixed layer, J. Geophys. Res., 100, 24691–24703, 1995. 1025
McPhee, M. G.: Ice-ocean momentum transfer for the AIDJEX ice model, AIDJEX Bull., 29, 93–111, 1975. 1027
Mellor, G. L. and Kantha, L.: An ice-ocean coupled model, J. Geophys. Res., 94, 10937–10954, doi:10.1029/JC094iC08p10937, 1989. 1024, 1025, 1028, 1029, 1043, 1046, 1047, 1048, 1049, 1065, 1066
Ou, H. W.: A time-dependent model of a coastal polynya, J. Phys. Oceanogr., 18, 584–590, doi:10.1175/1520-0485(1988)018<0584:ATDMOA>2.0.CO;2, 1988. 1034, 1035, 1038, 1055
Pease, C. H.: The size of wind driven polynyas, J. Geophys. Res., 92, 7049–7059, doi:10.1029/JC092iC07p07049, 1987. 1025, 1034, 1035, 1036, 1047, 1048, 1055
Semtner, A. J.: Model for thermodynamic growth of sea ice in numerical investigations of climate, J. Phys. Oceanogr., 6, 379–389, doi:10.1175/1520-0485(1976)006<0379:AMFTTG>2.0.CO;2, 1976. 1027
Smedsrud, L. and Skogseth, R.: Field measurements of Arctic grease ice properties and processes, Cold Reg. Sci. Technol., 44, 171–183, doi:10.1016/j.coldregions.2005.11.002, 2006. 1047
Smedsrud, L. H., Budgell, W. P., Jenkins, A. D., and Adlandsvik, B.: Fine-scale sea-ice modelling of the Storfjorden polynya, Svalbard, Ann. Glaciol., 44, 73–79, 2006. 1043

Tremblay, L.-B. and Hakakian, M.: Estimating the sea ice compressive strength from satellite-derived sea ice drift and NCEP reanalysis data, J. Phys. Oceanogr., 36, 2165–2172, doi:10.1175/JPO2954.1, 2006. 1031, 1032

Tremblay, L.-B. and Mysak, L. A.: Modeling sea ice as a granular material, including the dilatancy effect, J. Phys. Oceanogr., 27, 2342–2360, doi:10.1175/1520-0485(1997)027<2342:MSIAAG>2.0.CO;2, 1997. 1024, 1025, 1031

Walkington, I., Morales Maqueda, M. A., and Willmott, A. J.: A robust and computationally efficient model of a two-dimensional coastal polynya, Ocean Model., 17, 140–152, doi:10.1016/j.ocemod.2006.12.001, 2007. 1035

Willmott, A. J., Morales Maqueda, M. A., and Darby, M. S.: A model for the influence of wind and oceanic currents on the size of a steady state latent heat coastal polynya, J. Phys. Oceanogr., 27, 2256–2275, doi:10.1175/1520-0485(1997)027<2256:AMFTIO>2.0.CO;2, 1997. 1025, 1034, 1035

Winsor, P. and Björk, G.: Polynya activity in the Arctic Ocean from 1958 to 1997, J. Geophys. Res., 105, 8789–8803, doi:10.1029/1999JC900305, 2000. 1025, 1035, 1043, 1044, 1046, 1048, 1049

Table 1. Main physical parameters and constants used in the simulation.

Variable	Symbol	Value
ice density	ρ_i	930 kg/m^3
air drag coefficient	C_{da}	1.2×10^{-3}
water drag coefficient	C_{dw}	5.5×10^{-3}
ice strength parameters	C, P^*	30, 30 kN/m
ellipse axis ratio	e	2
min. viscosity (Hibler)	ζ_{min}	4×10^8 kg/s
max. viscosity (ellipse)	ζ_{max}	$(2.5\times10^8$ ms$)/P$
max. viscosity (mod. Coulomb)	ζ_{max}	$(10^6$ ms$)/P$
max. viscosity (granular)	η_{max}	10^{12} kg/s
internal angle of friction	ϕ	30°
angle of dilatency	δ	10°
air temperature	T_{air}	−20°C
cloud cover	F_c	80%
relative humidity	H_R	80%
wind speed, angle	$\|\boldsymbol{v}_a\|$, Θ	20 m/s, 30°
basin dimensions	L, W	135 km, 75 km
horizontal resolution	Δx	2.5 km
Coriolis factor	f	1.33×10^{-4} s^{-1}
ice demarcation thickness	h_0	30 cm

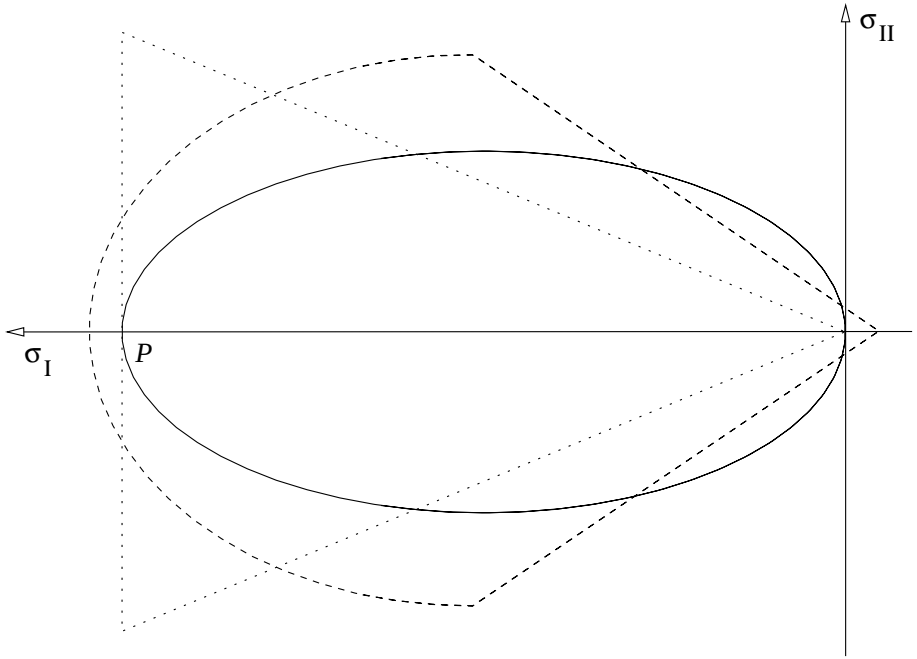

Fig. 1. The three yield curves discussed in the text; the elliptic, the modified Coulombic and the granular model's yield curves, depicted as solid, dashed and dotted lines, respectively. The yield curves are scaled against P or P_{max} as applicable.

TCD
3, 1023–1068, 2009

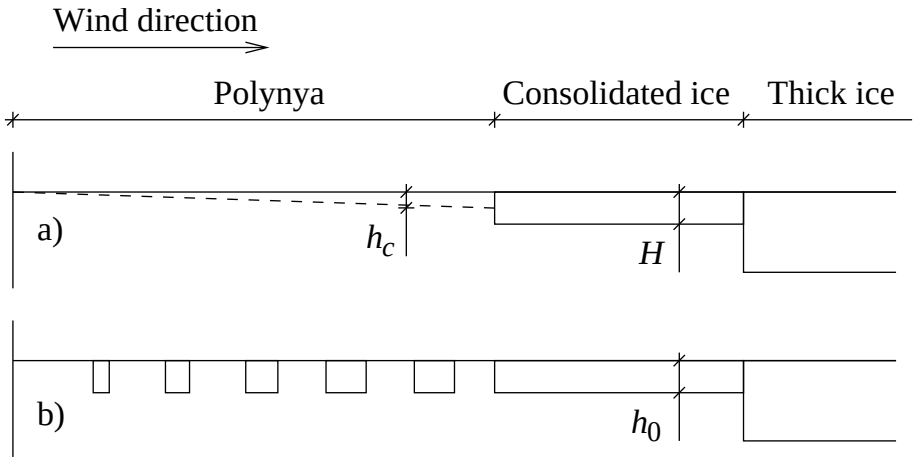

Fig. 2. Polynya formation in polynya flux models and a dynamic-thermodynamic sea-ice model. **(a)** In the Pease (1987) model frazil ice that is formed inside the polynya is immediately transported towards the thick ice. There it forms consolidated ice of thickness H. In the Ou (1988) model the frazil ice has finite drift speed inside the polynya and therefore also finite thickness h_c (dashed line). **(b)** In a dynamic-thermodynamic sea-ice model newly formed ice is immediately transformed into pancake ice of thickness h_0.

TCD
3, 1023–1068, 2009

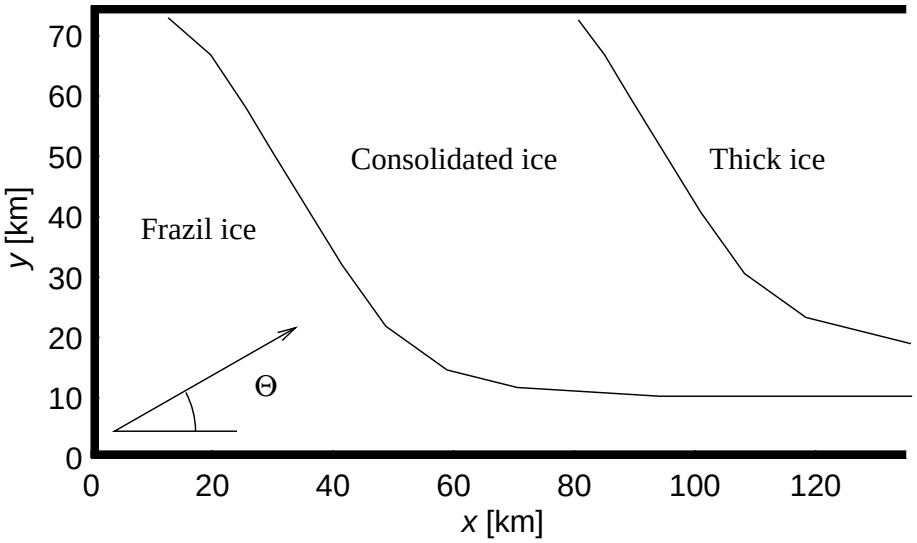

Fig. 3. The size of the basin (in km) and wind direction during the polynya experiments. The figure also shows the three ice regimes one expects; frazil/pancake ice, consolidated ice and thick initial ice.

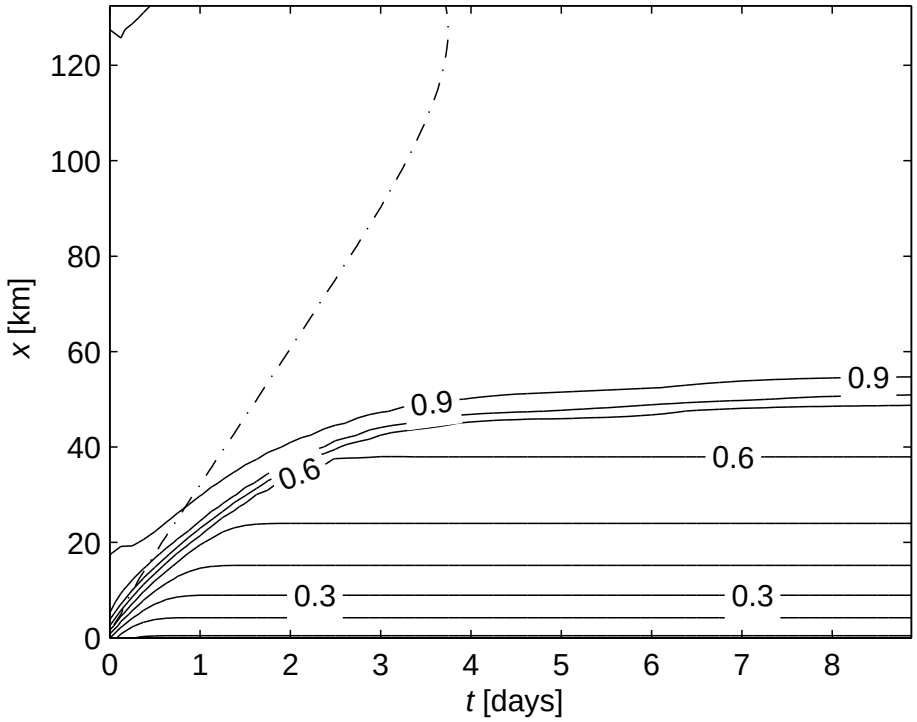

Fig. 4. A Hovmöller diagram of the ice concentration field in the control experiment taken along a section at y=37.5 km. The vertical axis (x) is the along channel distance and the horizontal axis (t) is the model time. The dash-dotted line shows the h=1 m isoline separating the thick initial ice and consolidated ice.

TCD
3, 1023–1068, 2009

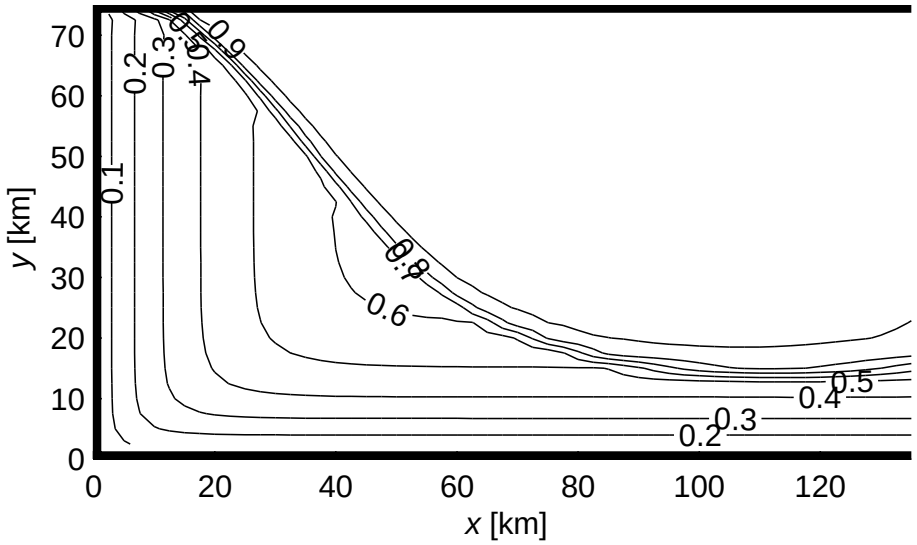

Fig. 5. Sea-ice concentration in the control experiment after eight days of model integration. The polynya edge is visible as a sharp increase in concentration.

TCD
3, 1023–1068, 2009

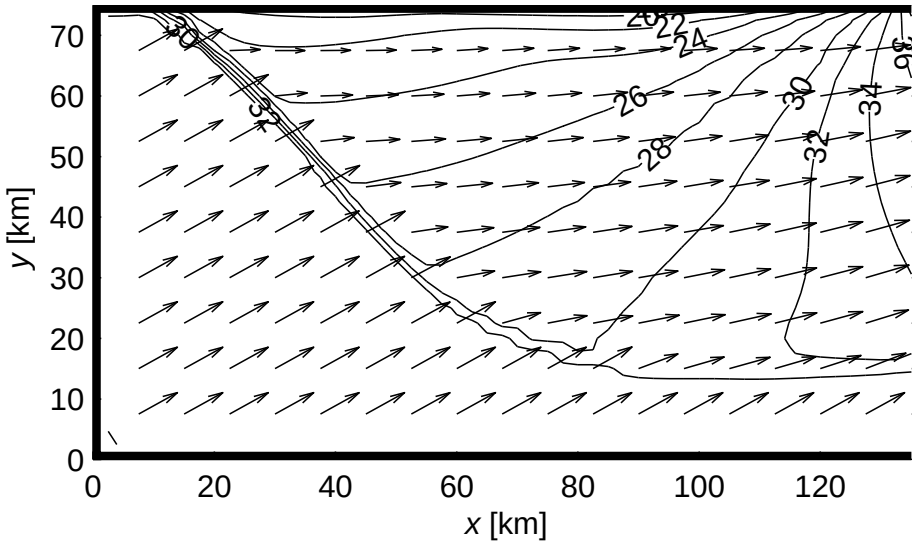

Fig. 6. Ice velocity and speed in the control experiment after eight days of model integration. The polynya edge is visible as a sharp decrease in the ice velocity.

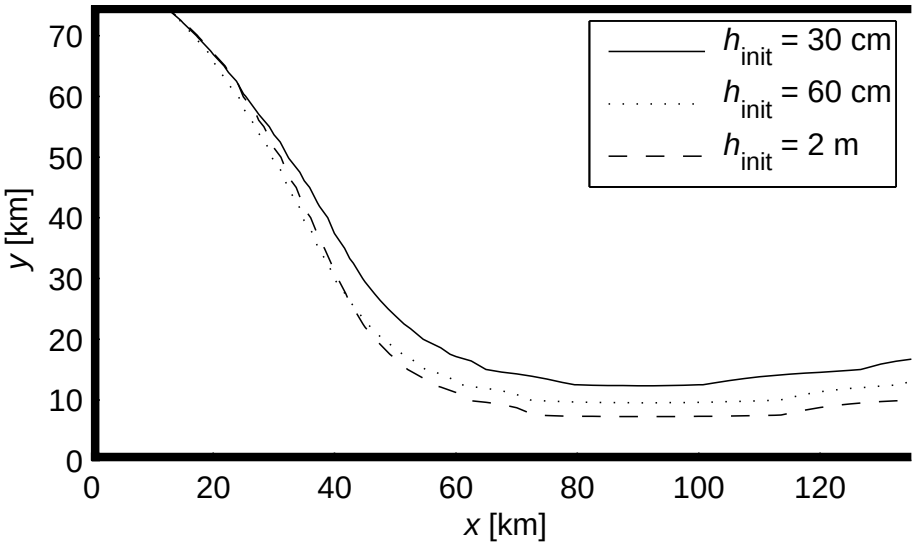

Fig. 7. The polynya edge (A=0.8) after two days of model integration starting from initial ice thickness of 30 cm, 60 cm and 2 m. Thick ice is stronger, both in shear and compression resulting in a slightly larger polynya when the initial ice is thin.

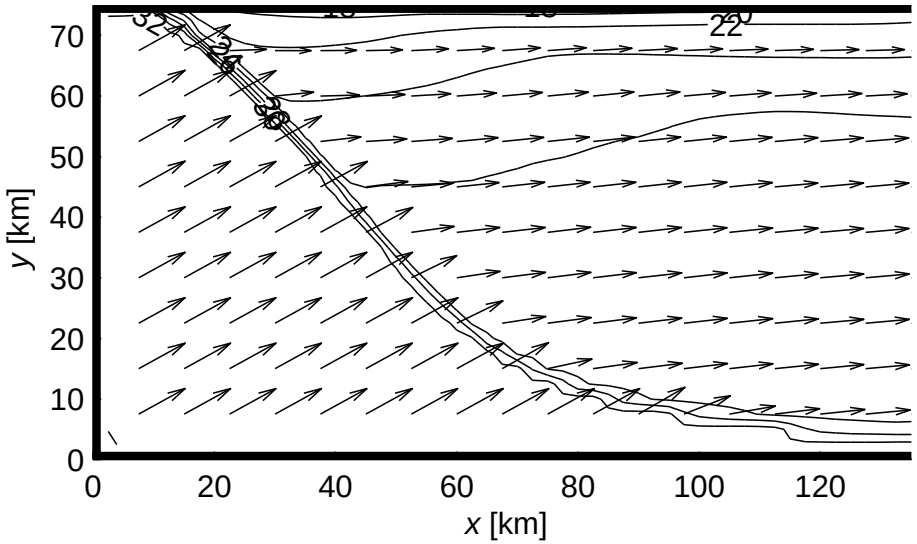

Fig. 8. Ice velocity and speed after eight days using $\partial P/\partial x=0$ at the open boundary. There is no sudden increase in velocity at the boundary as can be seen when using $P=0$ at the boundary (see Fig. 6).

TCD
3, 1023–1068, 2009

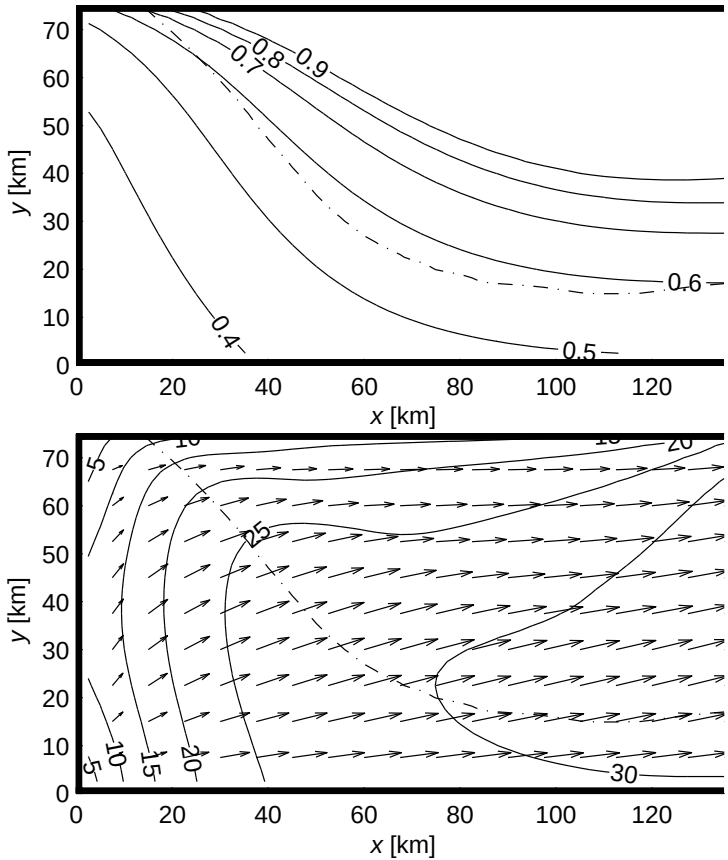

Fig. 9. Sea-ice concentration (top) and speed and velocity (bottom) using Hibler's original formulation for the elliptic yield curve, after eight days of model integration. Neither figure shows a discernible polynya edge. The dash-dotted line shows the isoline for A=0.8 from the control run.

TCD
3, 1023–1068, 2009

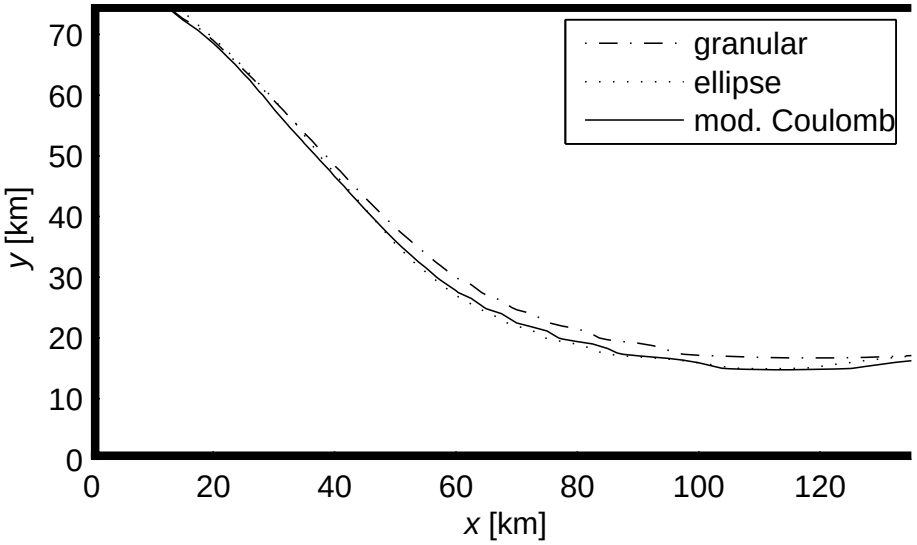

Fig. 10. The polynya edge (A=0.8) using the elliptic and modified Coulombic yield curves and the granular model after eight model days. The differences between different model formulations are minor.

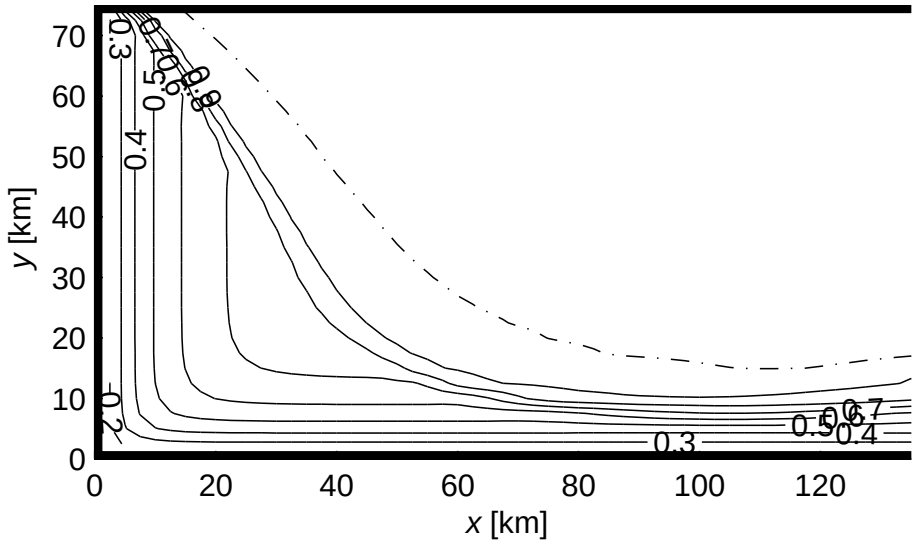

Fig. 11. The fractional ice concentration using h_0=10 cm after eight model days. The resulting polynya is smaller and has a higher ice concentration than the control run. The dash-dotted line shows the isoline for A=0.8 from the control run.

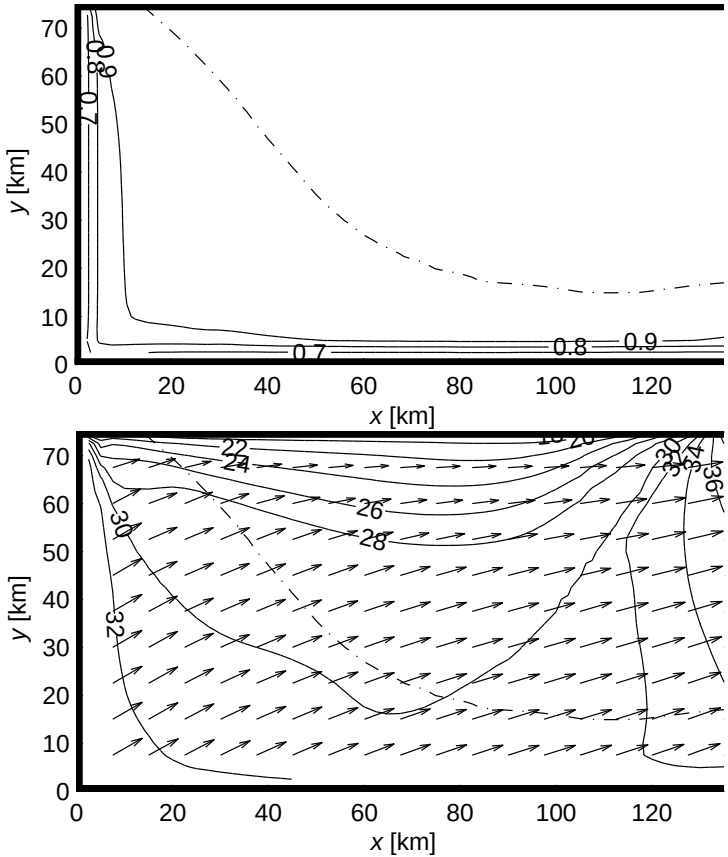

Fig. 12. The fractional ice concentration (top) and speed and velocity (bottom) using the approach by Mellor and Kantha (1989) after eight model days. The resulting polynya is very small with no discernible edge in the velocity field. The dash-dotted line shows the isoline for A=0.8 from the control run.

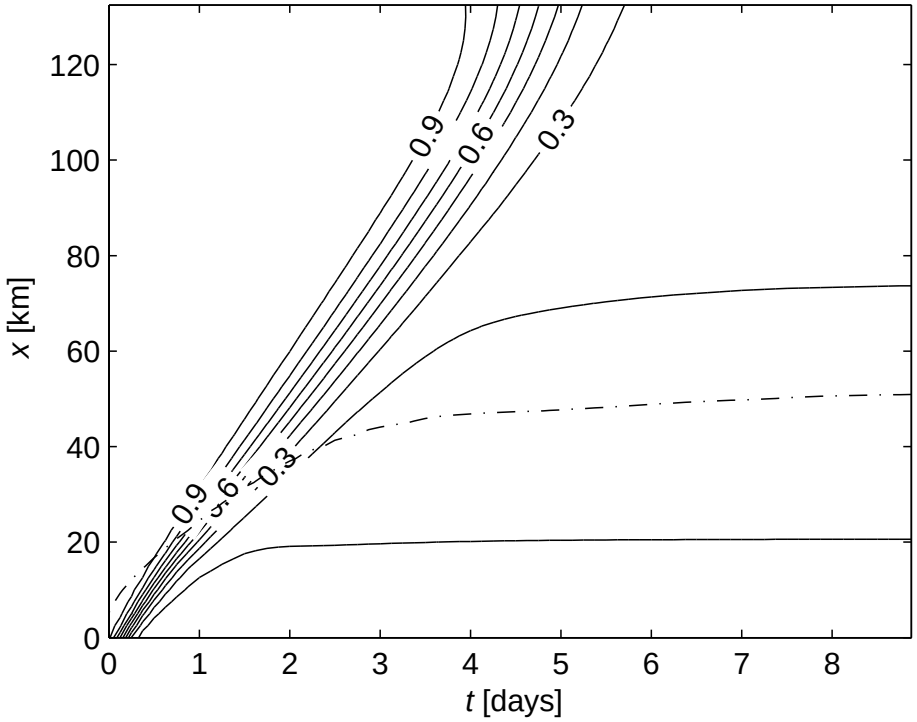

Fig. 13. A Hovmöller diagram of the ice thickness field using the new-ice thickness formulation by Mellor and Kantha (1989) taken along a section at y=37.5 km. The vertical axis (x) is the along channel distance and the horizontal axis (t) is the model time. The dash-dotted line shows the isoline for A=0.8 from the control run.

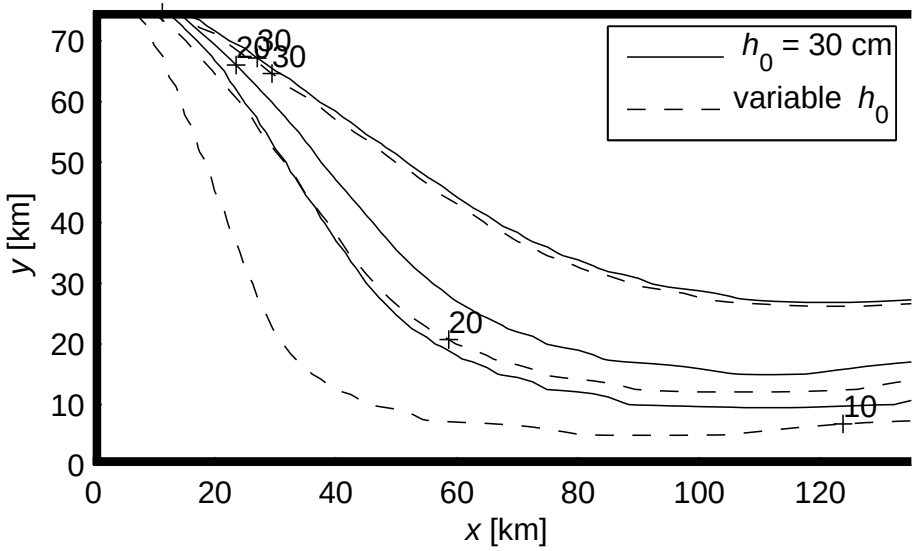

Fig. 14. The polynya edge after 8 days using a constant h_0 and parametrised h_0 according to Eq. (29). A=0.8 is used as a marker for the polynya edge and the edge is plotted for 10, 20 and 30 m/s wind speed.

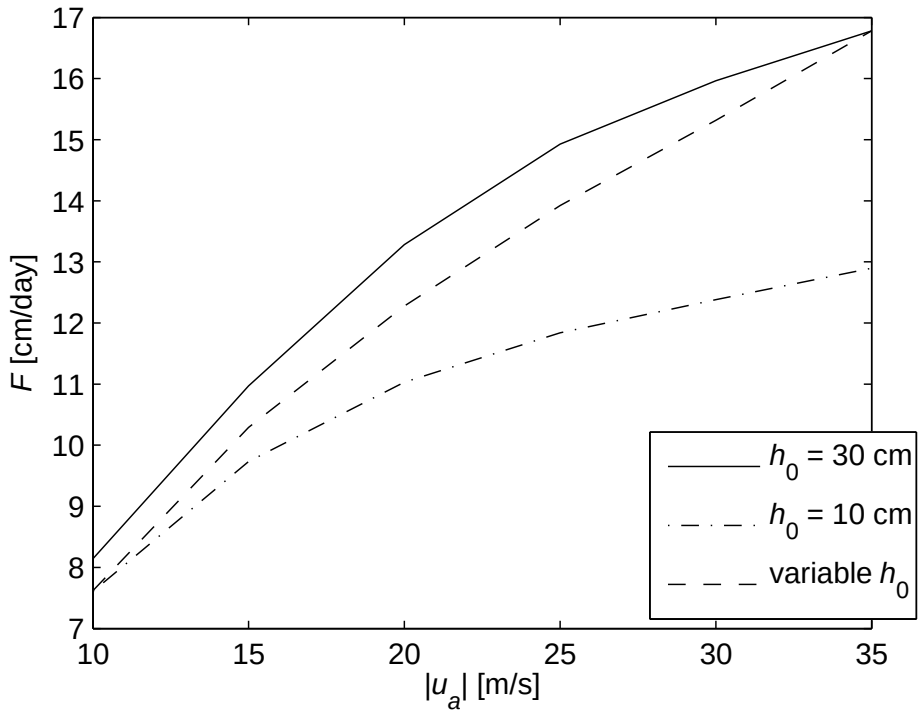

Fig. 15. Mean ice formation rate (F) in the polynya after 8 days as a function of wind speed. The mean ice formation rate is found by averaging the ice formation rate over all points where $A \leq 0.8$.